HHS Public Access

Author manuscript

Dev Biol. Author manuscript; available in PMC 2017 April 27.

Published in final edited form as:

Dev Biol. 2016 September 01; 417(1): 11–24. doi:10.1016/j.ydbio.2016.07.013.

Msx1 and *Msx2* function together in the regulation of primordial germ cell migration in the mouse

Jingjing Sun, **Man-Chun Ting**, **Mamoru Ishii**, and **Robert Maxson***

Department of Biochemistry and Molecular Biology, Norris Cancer Hospital, University of Southern California, Keck School of Medicine, 1441 Eastlake Avenue, Los Angeles, CA 90089-9176, USA

Abstract

Primordial germ cells (PGCs) are a highly migratory cell population that gives rise to eggs and sperm. Much is known about PGC specification, but less about the processes that control PGC migration. In this study, we document a deficiency in PGC development in embryos carrying global homozygous null mutations in *Msx1* and *Msx2*, both immediate downstream effectors of Bmp signaling pathway. We show that $Msx1^{-/-};Msx2^{-/-}$ mutant embryos have defects in PGC migration as well as a reduced number of PGCs. These phenotypes are also evident in a *Mesp1-Cre*-mediated mesoderm-specific mutant line of *Msx1* and *Msx2*. Since PGCs are not marked in *Mesp1*-lineage tracing, our results suggest that *Msx1* and *Msx2* function cell non-autonomously in directing PGC migration. Consistent with this hypothesis, we noted an upregulation of fibronectin, well known as a mediator of cell migration, in tissues through which PGCs migrate. We also noted a reduction in the expression of *Wnt5a* and an increase in the expression in *Bmp4* in such tissues in $Msx1^{-/-};Msx2^{-/-}$ mutants, both known effectors of PGC development.

Keywords

Primordial germ cell; PGC; Msx1, Msx2; Bmp pathway; Wnt5a; PGC migration; Fibronectin

1. Introduction

PGCs are the embryonic precursors of oocytes and spermatozoa. In mouse, PGCs are specified by a mechanism in which germline cells are induced from pluripotent epiblast cells by signaling molecules of the Bmp and Wnt families (Lawson et al., 1999; Ohinata et al., 2009; Ying et al., 2001; Ying and Zhao, 2001). Wnt3 causes epiblast cells in the pre-streak egg cylinder to become competent to adopt a PGC fate when supplied with Bmp4 (Ohinata et al., 2009). Bmp/Smad signaling allows the binding of mesodermal factor *T* (*Brachyury*), an effector of Wnt3, to *cis*-regulatory elements and activates *Blimp1* and *Prdm14*, two master transcriptional regulators that mark PGC precursors and coordinate a program of PGC specification (Aramaki et al., 2013; Magnusdottir et al., 2013; Nakaki et al., 2013; Ohinata et al., 2005; Yamaji et al., 2008). Bmp signaling plays an indirect role mediated by

*Corresponding author: maxson@usc.edu (R. Maxson).

its downstream transcription factors (TFs) in this process, by either repressing Wnt targets that inhibit *Blimp1* and *Prdm14* or activating coactivators that facilitate their activation (Aramaki et al., 2013).

During development, PGCs take a long journey that is highly coordinated with the morphogenesis of the tissues they pass through. Successful migration of PGCs requires both intrinsic signals that ensure PGC motility and survival (*Steel* factor or *Kitl*, *E-Cdh*, *Ror2*, *Wnt5a* (Chawengsaksophak et al., 2012; Di Carlo and De Felici, 2000; Gu et al., 2009; Laird et al., 2011)) and external guidance cues, attractive and repulsive (Molyneaux and Wylie, 2004; Richardson and Lehmann, 2010). Prior to migration, PGC founders are located at the allantois base. Around E7.75, PGCs exit the allantois mesoderm, enter the definitive endoderm and are carried along with the endodermal cells as the hindgut elongates (Anderson et al., 2000; Ginsburg et al., 1990). At E9.5, PGCs rapidly exit the basal lamina of the gut epithelium into the mesentery at E9.5. They move dorsally, reaching the dorsal body wall at E10.5 and migrate laterally into the genital ridge by E11.5 (Molyneaux and Wylie, 2004; Molyneaux et al., 2001).

Besides the chemoattraction mediated by Sdf1/Cxcr4 (Ara et al., 2003; Molyneaux et al., 2003), adhesion molecules and extracellular matrix (ECM) components provide a permissive environment for migrating PGCs (Anderson et al., 1999; Bendel-Stenzel et al., 2000; Di Carlo and De Felici, 2000; Diez-Torre et al., 2013). Disrupting β1-integrin results in impaired PGC-ECM interaction, and leads to extra-gonadal localization of PGCs (Anderson et al., 1999). Consistent with the requirement for integrins, glycoproteins in the ECM, such as Fibronectin, Laminin and Type IV collagen have been shown to interact with PGCs *in vivo* or *in vitro* (Alvarez-Buylla and Merchant-Larios, 1986; De Felici and Dolci, 1989; Fujimoto et al., 1985). Moreover, their adhesion to PGCs changes as a function of the developmental stages at which PGCs are isolated (De Felici et al., 1992; Ffrench-Constant et al., 1991; Garcia-Castro et al., 1997). ECM deposition is regulated by a number of cytokines of the TGF-β super family via Smads (Chuva de Sousa Lopes et al., 2005; Costello et al., 2009). In particular, Bmp4 enhances Fibronectin synthesis or assembly in a number of cell types (Molloy et al., 2008; Pegorier et al., 2010; Tang et al., 2003). *In vivo*, P-Smad1/5 is detected in the somatic mesodermal tissues surrounding migrating PGCs and Bmp4 stimulates the motility of migrating PGCs through its downstream TFs in organ culture (Dudley et al., 2007).

Msx genes encode highly conserved homeobox-containing transcription factors (Bell et al., 1993; Gauchat et al., 2000; Pollard and Holland, 2000). In mammals, *Msx1* and *Msx2* are expressed in overlapping domains and function cooperatively in controlling tissue interactions in many morphogenetic processes (Chen et al., 2007; Han et al., 2007; Ishii et al., 2005; Lallemand et al., 2005; Le Bouffant et al., 2011; Phippard et al., 1996; Roybal et al., 2010). They are well-documented immediate downstream effectors of the Bmp signaling pathway (Bei and Maas, 1998; Brugger et al., 2004; Furuta and Hogan, 1998; Marazzi et al., 1997; Vainio et al., 1993). In a survey of *Msx* gene expression during embryogenesis, we found that *Msx1* and *Msx2* are among the first group of mesodermal transcription factors activated by Bmps, as also suggested by another group (Aramaki et al., 2013; Kurimoto et al., 2008). This finding, together with the key role played by Bmp signaling in PGC

development prompted us to investigate whether *Msx* genes are involved in PGC development.

In this study, we show that *Msx1* and *Msx2* are expressed both in PGC precursors and in neighboring somatic cells, and that both conventional inactivation of *Msx1* and *Msx2*, as well as conditional ablation in the mesoderm, affect the initial step of PGC migration, resulting in an altered distribution of PGCs in the endoderm and ectopic localization of PGCs in the tail. We show that Msx1 and Msx2 function in the mesoderm upstream of Wnt5a and Bmp4, and present evidence for their influence on the distribution of Fibronectin and thus the migration of PGCs.

2. Materials and methods

2.1. Mice and genotyping

The generation and genotyping of classical and conditional *Msx1* and *Msx2* mutant alleles were reported previously (Fu et al., 2007; Satokata et al., 2000; Satokata and Maas, 1994). Classical mutant lines were maintained in a BALB/c genetic background, and compound *Msx1, Msx2* heterozygotes were crossed to produce $Msx1^{-/-};Msx2^{-/-}$ mutant embryos. Conditional *Msx1* and *Msx2* mutant alleles were maintained in mixed background. *Mesp1-Cre* and $R26R^{lacZ}$ allele was introduced to create the mesodermal-specific knockout embryos carrying a *lacZ* reporter (Saga et al., 1999; Soriano, 1999). *Mesp1-Cre;*$Msx1^{fl/fl};Msx2^{fl/fl};R26R^{lacZ/lacZ}$ mutants were generated through the mating between *Mesp1-Cre;* $Msx1^{+/fl};Msx2^{fl/fl};R26R^{lacZ/lacZ}$ males and $Msx1^{fl/fl};Msx2^{fl/fl};R26R^{lacZ/lacZ}$ females. The noon copulation plug was counted as embryonic day 0.5. Genomic DNA samples were prepared from mouse tails for adults or embryonic tissues according to the method reported by Hogan et al. (1994).

2.2. cDNA synthesis and qPCR

Total RNA was extracted from the caudal part of E11.5 mouse embryos with RNeasy plus mini kit (Qiagen). The first strand cDNA was synthesized with Omniscript RT kit (Qiagen). For each reverse transcription product, the following primers were used for qPCR analysis: *Fibronectin*, 5′-TAC CAA GGT CAA TCC ACA CCC C-3′ (forward), 5′-CAG ATG GCA AAA GAA AGC AGA GG-3′ (reverse); *Gapdh*, 5′-ACC ACA GTC CAT GCC ATC AC-3′ (forward), 5′-TCC ACC ACC CTG TTG CTG TA-3′ (reverse). The relative expression levels were normalized by *Gapdh* mRNA level. Student *T*-test was used to evaluate the significance.

2.3. In situ hybridization

An *Msx1* 1.2kb XhoI-XbaI cDNA fragment was subcloned into pSP72. *Msx2* full-length cDNA was cloned into pBSKII(+) between BamHI and EcoRI sites. The *Blimp1* cDNA construct is a kind gift from Dr. Saitou at RIKEN Kobe Institute, Japan (Ohinata et al., 2005). The Fragilis cDNA probe was obtained from Dr. Surani at Wellcome Trust/Cancer Research UK Institute (Saitou et al., 2002). The *Wnt5a* probe was generously provided by Dr. SK Dey at Cincinnati Children's Hospital Medical Center (Daikoku et al., 2011). A 700bp *Fibronectin* cDNA probe was generated by PCR with forward 5′-AGA TGA CTC

ATG CTT TGA CCC-3′ and reverse 5′-TGC TGA AGC TGA GAA CAT GGC-3′ primers. Ribonucleotide probes were synthesized by PCR with either Fluorescein-UTP or Digoxygenin-UTP (Roche Applied Science). Whole-mount *in situ* hybridization was performed largely based on the method reported by Hogan and visualized by BM-purple substrate (Roche Applied Science) (Hogan et al., 1994). Prior to sectioning, embryos were fixed overnight in 4% PFA/PBS and embedded in HistoPrep (Fisher). *In situ* hybridization on frozen sections was performed as previously described and fluorophore-conjugated Tyramide (TSA™PLUS, Perkin Elmer) was used to amplify the signal (Ting et al., 2009).

2.4. β-Galactosidase and alkaline phosphatase staining

For β-Gal staining on frozen sections, 0.2% glutaraldehyde/PBS was used for fixation prior to staining. Sections were then washed and stained overnight at 37 °C as previously described (Ishii et al., 2003). To count PGCs at E8.5, embryos were dissected and fixed for 1 h in 4% PFA/PBS at 4 °C, washed three times in cold PBS and treated with 70% ethanol for 1 h at 4 °C. After washing another three times with distilled water, they were stained with α-naphthyl phosphate/fast red TR for 15 min at room temperature (Ginsburg et al., 1990). Embryos were then rinsed in water and preserved in 70% glycerol. The anterior portion of each embryo was collected for genotyping, and the posterior portion was flattened under a coverslip for counting. Alkaline phosphatase staining on frozen sections was performed according to the method reported previously (Ishii et al., 2003).

2.5. Immunohistochenistry

To evaluate cellular proliferation at E11.5, BrdU (Sigma) was injected into the pregnant female (200 μg/g body weight) 2 h prior to dissection. Immunodetection was done with a BrdU staining Kit (Life Technologies) following alkaline phosphatase staining. A rabbit anti-PH3 antibody (1:200, upstate) and a mouse anti-SSEA-1 antibody (1:200, Developmental Studies Hybridoma Bank) were used for double labeling at E12.5. To detect Fibronectin, a polyclonal anti-Fibronectin antibody (1:200, Sigma) was used. Rhodamine or FITC conjugated anti-mouse IgG or anti-rabbit IgG secondary antibodies were used for immunofluorescent detection and DAPI for counterstaining. For polyclonal rabbit β-Gal antibody (Cappel, MP Biomedicals), a peroxidase conjugated goat anti rabbit IgG secondary antibody (Life Technologies) was used to activate the fluorescein conjugated tyramide (TSA™PLUS, Perkin Elmer).

2.6. Quantification and statistics

For PGC counting at E8.0–8.5, all the embryos harvested and stained (n=181) were first categorized by their genotypes and numbers of somite. Number of PGCs counted from embryos at 4–9 (n=73) somite stage were plotted because at least one *Msx1*$^{-/-}$*; Msx2*$^{-/-}$ mutant embryo was obtained. A standard deviation was calculated if there were more than one individual in the category. Three pairs of *Msx1*$^{+/-}$ (one female and two males) and *Msx1*$^{-/-}$*; Msx2*$^{-/-}$ (three males) embryos were harvested to compare number of PGCs at E12.5. After frozen sectioning and ALP staining, numbers of PGCs in the genital ridge, the mesentery and dorsal body wall as well those in the tail were calculated separately by adding up the counts from each transverse section through the posterior portion of the embryos. 135, 145 and 130 sections from *Msx1*$^{+/-}$ controls were counted; among these 103, 110 and

95 sections respectively were cut through the genital ridges. From *Msx1*$^{-/-}$;*Msx2*$^{-/-}$ mutants, 165, 220 and 175 sections were counted, and 91, 98 and 90 through the gonads. The comparison between the control and *Mesp1-Cre* conditional *Msx1, 2* mutant embryos were done in the same manner (one female and two males for both genotypes). To calculate the proliferation index of PGCs in the gonad, PH3/SSEA-1 double immunostaining was done in one pair of control and mutant embryos (both males) at E11.5 and two pairs at E12.5, and ALP/BrdU staining was performed with two pairs of E11.5 embryos. All the sections obtained from one individual were counted and an index was calculated by averaging the percentage of PH3 or BrdU-positive PGCs on each that contains more than ten PGCs. Data shown was from one pair of ALP/BrdU double stained control and mutant, in which 66 and 53 sections were taken into counting and over 900 and 850 PGCs were counted. The student *t*-test was used to evaluate the significance.

3. Results

3.1. Msx1 and Msx2 are expressed in the tissues that give rise to PGCs

Typically 6 Blimp1-positive PGC precursors are induced from the posterior proximal epiblast at E6.25, increasing to approximately 16 by E6.5 (Ohinata et al., 2005). These cells give rise to the 45 *Fragilis*-positive founder PGCs at E7.25 (Saitou et al., 2002). We carried out *in situ* hybridization to determine the expression domains of *Msx1 and Msx2* in relation to the location of PGCs. Using both whole mounts (Fig. 1A–F) and sections (Fig. 1G–I″), we found that *Msx1* was expressed in the distal end of the primitive streak (arrows, Fig. 1A, G) and visceral endoderm (VE) (arrowheads, Fig. 1A, G) at E6.5. *Msx2* transcripts were detectible only in tissue of mesodermal origin (arrows, Fig. 1D, G′).

At approximately E7.5, both *Msx1* and *Msx2* were expressed in the embryonic and extraembryonic mesoderm, including the allantois (asterisks, Fig. 1B, E, H–H″, I–I″), amniotic mesoderm and some chorionic mesoderm. The expression of both genes became even stronger at E8.0 (Fig. 1C, F). *Msx1* was maintained in the VE during the relocation of PGCs from the allantois base to the gut endoderm (arrowhead, Fig. 1I).

Msx genes were thus continuously expressed in the tissues that contain PGCs or their precursors. The expression of *Msx* genes is likely induced by Bmp signaling at the time of PGC specification. A *lacZ* reporter driven by a 560 bp distal *Msx2* enhancer fragment, *560bpMsx-hsplacZ* was expressed in the proximal epiblast at E6.25 and became restricted to the posterior primitive streak from E6.5 (Supplementary Fig. 1A, B, D–F). This enhancer element responds to Bmp signaling efficiently *in vivo* and *in vitro* through a central AT-rich *Antennapedia*-class homeodomain recognition sequence flanked by Smad-binding sites (Brugger et al., 2004). A mutation in the AT-rich site that abolishes the Bmp-responsiveness of this element also eliminated its expression in the egg cylinder (Supplementary Fig. 1C), suggesting that Bmp signaling activates *Msx2* in the epiblast.

To determine whether *Msx* genes are expressed in PGCs, we labeled frozen sections of embryos at E6.5 to E8.5 with an *Msx1* or *Msx2* probe and a *Blimp1* or *Fragilis* probe simultaneously, and visualized the signals by immunofluorescence microscopy. Double labeling with *Blimp1 and Msx1/2* revealed some punctate yellow pixels at E6.5 and E7.75

(arrows, Fig. 2A–D′), indicating coexpression of these mRNAs. Transcripts of *Msx*1 and *Msx2* were clearly more concentrated in mesoderm and VE surrounding PGC precursors or founders. We obtained a similar result with a *Fragilis* probe at E7.5 (Fig. 2E–F′).

At E8.5, *Msx1* was expressed in the allantois, extraembryonic visceral endoderm (ExVE) and gut endoderm (Fig. 2G). *Fragilis*-marked PGCs are embedded in the endoderm, transitioning from ExVE to gut endoderm. Though *Msx1* was expressed in the surrounding endoderm, no signal was observed in PGCs. *Msx2* was not expressed significantly in the endoderm (Fig. 2I). At E9.5, a majority of PGCs are migrating anteriorly along the hindgut, and both *Msx1* and *Msx2* transcripts were found in the body wall. Collectively, *Msx1* and *Msx2* were expressed in PGC precursors and PGC founders at low levels, but were subsequently excluded from endoderm-localized PGCs by E8.5. Our results are consistent with a previous single-cell array analysis suggesting that *Msx1* and *Msx2* are upregulated in *Blimp1*-positive PGCs isolated from E/MB-stage (E7.25–E7.5) embryos compared to PS-stage (E6.25) proximal epiblast (PrE) cells (Kurimoto et al., 2008).

3.2. Loss of function of Msx1 and Msx2 causes a defect in PGC migration

Knowing that *Msx* genes are expressed in the tissues that give rise to PGCs, we asked whether loss of *Msx* gene function causes any deficiency in germ cell development. We carried out whole mount ALP staining to identify PGCs within E8.0–8.5 embryos produced by $Msx1^{+/-};Msx2^{+/-}$ parents. In wild-type and controls, PGCs were first located in the junction of the allantois and gut endoderm (Fig. 3B), and then along the invaginating hindgut (Fig. 3C). Both the active migration by PGCs themselves and the expansion of hindgut endoderm may contribute to this relocation process (Anderson et al., 2000; Hara et al., 2009). $Msx1^{-/-};Msx2^{-/-}$ mutants contained PGCs, suggesting that *Msx* genes are not absolutely required for PGC specification. However, the distribution of PGCs in gut endoderm was abnormal. In the 4-somite mutant embryo, a string of PGCs stretched along the most posterior end of the endoderm (Fig. 3D). More strikingly, these PGCs formed several parallel strings across the hindgut endoderm at the 8-somite stage (Fig. 3E). PGCs in $Msx1^{-/-};Msx2^{-/-}$ mutants were thus spread laterally instead of being confined to the hindgut in the middle. This phenotype is not due to a change in the timing of when PGCs leave the allantois mesoderm and enter the endoderm, as this occurred in both control and mutant embryos at approximately E7.5 (Supplementary Fig. 2A–E).

We proceeded to examine the distribution of PGCs at E9.5 when they are migrating anteriorly along the hindgut epithelium and dorsally throughout the mesentery towards the dorsal aorta. The posterior portions of both control and mutant embryos were sectioned and subjected to ALP staining. We compared the sections from control and mutant embryos at similar levels along the A–P axis and found that PGC migration was retarded in the mutants. In $Msx1^{+/-}$ controls, more PGCs were found in the anterior hindgut region (Fig. 3G), and no PGCs were left in the very end of the tail (Fig. 3I). In $Msx1^{-/-};Msx2^{-/-}$ mutants, fewer PGCs reached the anterior hindgut (Fig. 3J) and a few clusters of PGCs were found at the posterior hindgut region (arrow, Fig. 3L). Some tail-localized PGCs in the mutants were not incorporated into the hindgut epithelium (Fig. 3O), and therefore were not on the path to the gonad. We also saw a delay in migration and ectopic location of PGCs in the tail in whole

mount stained embryos (arrowheads, Supplementary Fig. 2J, K). At E11.5, a number of PGCs were still present in the tails of *Msx1*$^{-/-}$;*Msx2*$^{-/-}$ mutants (Fig. 3P).

Although the majority of PGCs reached the genital ridge by E12.5, a small number were still migrating through the dorsal mesentery in wild-type or *Msx1*$^{+/-}$ control embryos. However, this process was greatly delayed in *Msx1*$^{-/-}$;*Msx2*$^{-/-}$ mutants. We counted the number of PGCs located in the mesentery and dorsal body wall in both control and mutant embryos, and found that in mutants, there was a significantly greater number of PGCs left in both sites (Fig. 3Q). Most strikingly, we observed a large number of mislocalized PGCs in the distal end of the tail (Fig. 3Q), a phenotype similar to one reported in mice deficient in the proapoptotic protein, Bax (Runyan et al., 2008; Stallock et al., 2003). Additional clusters of ectopic PGCs were found in the ventral body wall.

In summary, loss of *Msx1* and *Msx2* gene function resulted in a defect in PGC migration. Beginning with the aberrant distribution in the definitive endoderm at E8.0, continuing with the ectopic localization in the posterior end from E9.5, *Msx1*$^{-/-}$;*Msx2*$^{-/-}$ mutants not only exhibited an overall delay in PGC migration, but also contained significantly more PGCs that have failed to be incorporated into the hindgut and remained in the tail.

3.3. A reduced number of PGCs in Msx1$^{-/-}$;Msx2$^{-/-}$ mutant embryos

By examining sections stained for ALP, it was clear that both the size of the genital ridge and the number of PGCs residing in it were greatly reduced in E12.5 *Msx1*$^{-/-}$;*Msx2*$^{-/-}$ mutants (Fig. 4C, D). Counting PGCs in different locations, the number was reduced by approximately 30% compared to the control ($P<0.05$, Fig. 4B). We wished to understand the cellular basis of this defect. In particular, we wished to know whether this is a defect in PGC specification, a deficiency in proliferation or is a consequence of an effect on cell survival during PGC migration. We first collected embryos from E8.0 to E8.5, performed whole mount ALP staining and counted the number of PGCs in both mutants and controls. Among embryos with 4–8 somites, *Msx1*$^{-/-}$;*Msx2*$^{-/-}$ mutants contain fewer PGCs compared to embryos of other genotypes (Fig. 4A), suggesting that the function of *Msx* genes may contribute to establishing or maintaining the germline in prior to E8.0.

When assessed at E12.5, the reduction in the number of PGCs was smaller than when assessed at E8.5. This smaller reduction at E12.5 could be a result of increased PGC proliferation or decreased apoptosis in mutant embryos. With antibodies against both PH3 and BrdU, we detected an increase in mitotic activity among PGCs in the genital ridges in mutant embryos at E11.5 (arrows, Fig. 4E, F; $P<0.001$, Fig. 4G–I) and E12.5 (arrows, Supplementary Fig. 3I, J), possibly reflecting a compensatory mechanism within the gonad whose function is to maintain an appropriate number of germ cells. As indicated by anti-cleaved Caspase3, there were very few apoptotic cells within the gonads at E12.5 (Supplementary Fig. 3E, G). Many more PGCs were retarded in migration and were present in the mesentery in *Msx1*$^{-/-}$;*Msx2*$^{-/-}$ mutants. A few of these cells underwent apoptosis (arrows, Supplementary Fig. 3H). This small number of apoptotic cells suggests that it is not likely that apoptosis significantly affects the total number of PGCs at this stage.

3.4. Defects in PGC development in Msx1$^{-/-}$;Msx2$^{-/-}$ mutants are cell-nonautonomous

We have shown that *Msx1* and *Msx2* were initially expressed in the distal end of the primitive streak at the time of PGC induction. However, their expression was down-regulated in committed PGCs along with *Hoxb1* and other somatic mesodermal genes (Kurimoto et al., 2008). The migrating PGCs do not express *Msx1* or *Msx2* at detectable levels. Therefore, we hypothesized that *Msx* genes function non-autonomously in the surrounding mesodermal tissue regulating PGC development. To test this hypothesis, we created mesoderm-specific *Msx1, 2* knockout embryos by crossing the *Mesp1-Cre* allele (Saga et al., 1999) into *Msx1, 2*$^{fl/fl}$;*R26R*$^{LacZ/LacZ}$ mice (Fu et al., 2007; Soriano, 1999), and compared the PGC phenotype of such mice to the phenotype of the classical *Msx1, 2* knockout embryos.

During gastrulation, *Mesp1* is expressed in all mesodermal cells as they exit the primitive streak between E6.5 and E7, and is rapidly down-regulated after E7.5. As a result, *Mesp1-Cre* induces extensive recombination in a sub-population of mesoderm-derived tissues (Saga et al., 1996, 1999), including visceral mesoderm in direct contact with PGC-containing hindgut at E8.5 (Fig. 5D and E), which also expresses *Msx1* and *Msx2* (Fig. 5A–C).

To confirm that *Mesp1-Cre* inactivates *Msx* genes only in somatic tissue, we assessed the Cre activity of *Mesp1-Cre* at E12.5 and E13.5 in *Mesp1-Cre;R26R*$^{+/LacZ}$ embryos with an antibody against β-Galactosidase. A monoclonal SSEA-1 antibody was used to simultaneously identify the germ cells. In approximately 20 sections of the genital ridge, we did not find any co-localization of SSEA-1 with β-Galactosidase (Fig. 5F, G), suggesting that the *Msx1* and *Msx2* alleles were intact in the germline.

We then asked whether the distribution of PGCs was altered in *Mesp1-Cre;Msx1,2*$^{fl/fl}$ mutants in a manner similar to the conventional *Msx1, 2* mutants. With whole mount ALP staining, we found that relative to controls, *Mesp1-Cre*-specific *Msx1, 2* knockout embryos exhibited more laterally distributed PGCs at E8.0 (Fig. 5H, I) and more tail PGCs at E9.0 (Fig. 5J, K), resembling the conventional mutants. We also examined the defect at E12.5, performing ALP staining on frozen sections of E12.5 embryos. We found that 1) there were significantly more tail PGCs in *Mesp1-Cre;Msx1,2*$^{fl/fl}$ mutants than in their littermate controls (*Mesp1-Cre* negative) ($P<0.05$, arrows, Fig. 5L–N); 2) PGC migration was delayed in *Mesp1-Cre;Msx1,2*$^{fl/fl}$ mutants (Fig. 5O); 3) and the total number of PGCs in *Mesp1-Cre;Msx1,2*$^{fl/fl}$ mutants was reduced by 30% compared to the controls ($P<0.001$, Fig. 5P). These data suggest that the PGC phenotype of *Mesp1-Cre;Msx1,2*$^{fl/fl}$ mutant embryos is indistinguishable from that of *Msx1*$^{-/-}$;*Msx2*$^{-/-}$ mutants, at least before E12.5. Therefore, the PGC defect in the mutants is likely caused by cell nonautonomous effects of the loss of *Msx1, 2* function.

3.5. No change in Sdf1, Col4a1 and Mmp14, but altered expression of Wnt5a, Bmp4, and Fibronectin along the PGC migration pathway in Msx1$^{-/-}$;Msx2$^{-/-}$ mutants

Given the probable non-autonomous influence of *Msx1, 2* on PGC migration, we examined the expression of candidate chemokines and ECM molecules that might affect PGC migration in *Msx1*$^{-/-}$;*Msx2*$^{-/-}$ mutants. We first examined the expression of the chemokine

Sdf1 (Cxcl12) and its receptor *Cxcr4* in E9.5 embryos and found no obvious change (Supplementary Fig. 4A–D). This was confirmed by RT-PCR with caudal tissues isolated from E11.5 embryos (Supplementary Fig. 4E). It has been shown that Type I collagen deposited around the hindgut is regulated by TGF-β signaling *via* Alk5, thus facilitating the migration of PGCs along the basal lamina (Chuva de Sousa Lopes et al., 2005). However, in *Msx1*$^{-/-}$;*Msx2*$^{-/-}$ mutants, the distribution of Type I collagen in the ECM appeared to be unaltered (data not shown). Nor did we detect changes in the levels of *Col4a1* and *Mmp14* mRNA (Supplementary Fig. 4E).

A previous study showed that *Wnt5a-Ror2* signaling promotes directional migration of PGCs in response to Kitl (Laird et al., 2011). Interestingly, loss of function of *Ror2* or *Wnt5a* leads to a PGC migration defect resembling the one we observed in *Msx1*$^{-/-}$;*Msx2*$^{-/-}$ mutants, although this defect is more severe than the *Msx1*$^{-/-}$;*Msx2*$^{-/-}$ phenotype (Chawengsaksophak et al., 2012; Laird et al., 2011). In both cases, migration of PGCs is disrupted when they move rostrally along the hindgut and dorsally through the mesentery at E10.5, resulting in a significant reduction in the number of PGCs arriving at the genital ridge and an increase in the number remaining in the gut mesentery and the tail including surface ectoderm.

Knowing that Msx proteins can bind directly to *cis*-regulatory sequences of *Wnt5a* and regulate its transcription *in vitro* and *in vivo* (Daikoku et al., 2011; Huang et al., 2005; Iler and Abate-Shen, 1996), we investigated the effect of loss of *Msx1, 2* function on the *Wnt5a-Ror2* pathway. Indeed, we found that *Wnt5a* was expressed in the hindgut mesentery at a much lower level in *Msx1*$^{-/-}$;*Msx2*$^{-/-}$ mutant embryos compared to the controls at E9.5 (Fig. 6D, E), suggesting that *Msx1* and *Msx2* function upstream of this pathway.

Though well-documented as Bmp targets, *Msx* genes are also known to function upstream of the Bmp pathway (Bei and Maas, 1998; Ishii et al., 2005; Sun et al., 2013). Given that P-Smad1/5 is detected in the somatic mesodermal tissues surrounding migrating PGCs, we hypothesized that Bmp4 might be altered in *Msx1, 2* mutants along the PGC migration pathway. Consistent with this possibility, we noted a clear increase in the level of *Bmp4* mRNA in the body wall and surface epithelium of the genital ridge in *Msx1, 2* mutants (arrows, Fig. 6G, I).

Bmp4 enhances Fibronectin synthesis or assembly in a number of cell types (Molloy et al., 2008; Pegorier et al., 2010; Tang et al., 2003), and Fn is a critical substrate for migrating PGCs (De Felici and Dolci, 1989; Ffrench-Constant et al., 1991; Garcia-Castro et al., 1997). The adhesiveness of PGCs to Fn decreases through development, and is completely lost upon the arrival of PGCs at the genital ridge (Ffrench-Constant et al., 1991), suggesting the adhesion of PGCs to Fn as well as, Fn concentration, are crucial and tightly regulated. We therefore examined Fn distribution in *Msx1, 2* mutant embryos. By using an anti-Fn antibody, we detected an upregulation of Fn in *Msx1*$^{-/-}$;*Msx2*$^{-/-}$ mutants compared to controls from E8.5 to E11.5 (Fig. 7). In particular, expression of Fn in the basement membrane of gut endoderm at E8.5 (Fig. 7A–B′) and in the hindgut and dorsal mesentery from 9.5 to E11.5 (Fig. 7C–H′) was upregulated in the mutants. During PGC migration, Fn is highly concentrated in the mesentery that connects gut to the dorsal midline of primitive

genital ridges, where migrating PGCs are clearly in contact with Fn. We suggest that this increase in Fn expression in the mutants could alter the balance between attachment and de-attachment of PGCs, thus interfering with their migration.

4. Discussion

We show that global inactivation of *Msx1* and *Msx2* in mice resulted in a reduction in the number of primordial germ cells as well as deficiencies in their migration. We observed similar phenotypes in conditional mutants in which *Msx1* and *Msx2* were inactivated in a subset of mesodermal cells by means of *Mesp1-Cre*, suggesting that *Msx* genes function non-autonomously in the control of primordial germ cell development.

PGCs are induced by the synergistic actions of Bmp4, Bmp2 and Bmp8b (Lawson et al., 1999; Ying et al., 2000; Ying and Zhao, 2001). The activity of Wnt3a precedes Bmps and prepares the cells in the epiblast for the action of Bmps (Ohinata et al., 2009). While *Msx* genes are targets of both Bmp and Wnt signaling pathways (Bei and Maas, 1998; Hussein et al., 2003; Marazzi et al., 1997; Vainio et al., 1993; Willert et al., 2002), Bmp signaling is likely responsible for *Msx* gene activation in the epiblast. In *Wnt3*$^{-/-}$ epiblast-like cells, exogenous Wnt3A does not induce transcription of *Msx2*; and Bmp4 or Bmp4 and Wnt3A together activate *Msx2* to a similar degree (Aramaki et al., 2013). Also supporting a key role for the Bmp pathway in *Msx2* activation is our observation that a mutation in a Bmp-responsive *Msx2* enhancer element (*560bpMsx2-hsplacZ*) known to disrupt *Msx2*'s Bmp-responsiveness (Brugger et al., 2004) also abolishes its expression in the proximal epiblast and the distal primitive streak (Supplementary Fig. 1).

It was previously reported that *Msx1* and *Msx2* are among a group of mesodermal transcription factors that are upregulated in committed PGCs in E7.25 embryos (*Blimp1*-positive, *Hoxb1*-negative) compared to proximal epiblast cells in E6.25 embryos (Kurimoto et al., 2008). These transcription factors, including *T*, *Cdx2*, *Id1*, *Hand1* and *Nkx1–2*, are normally associated with the formation of nascent mesoderm. With *in situ* hybridization, we detected *Msx1* and *Msx2* transcripts in tissues that give rise to the germ cell lineage. These transcripts co-localize partially with *Blimp1* and *Fragilis* transcripts (Fig. 2), suggesting that *Msx1* and *Msx2* are expressed in a subset of germline cells at the time of PGC specification.

Mesodermal factor *T,* induced by Wnt3a, directly activates *Blimp1* and *Prdm14* in the germline (Aramaki et al., 2013). This process requires Bmp4. This function of Bmp4 may be mediated by its immediate downstream effectors working together with T to activate *Blimp1* expression. That Bmp4 treatment stimulates the transcription of *Msx2* more rapidly than *Blimp1* (Aramaki et al., 2013) suggests that although *Msx* genes are not strictly required to specify PGC fate, they are part of the gene regulatory network that establishes the germline and mesoderm lineages during gastrulation. By E8.25, *Msx* genes are downregulated in PGCs but maintained in mesoderm (Fig. 2G–J).

Both global and *Mesp1-Cre*-mediated conditional *Msx1, 2* mutant embryos contain significantly fewer ALP-positive PGCs than do controls (Figs. 4B and 5P). This decrease in the numbers of PGCs is evident as early as E8.0 (Fig. 4A). Our finding that there is no

increase in the numbers of PGCs in extraembryonic tissues of the mutants (data not shown) led us to hypothesize that *Msx1* and *Msx2* function non-autonomously in the mesoderm, particularly in the posterior streak and allantois, as part of the process that provides a proper niche for the population expansion of pre-migratory PGCs. From E8.25 to E12.5, the reduction in the numbers of PGCs in the *Msx1, 2* mutants drops from 40–60% to 30%, suggesting that a compensatory mechanism drives the proliferation of PGCs in the genital ridge of $Msx1^{-/-};Msx2^{-/-}$ mutants (Fig. 4G–I), rescuing the deficiency in germ cell number. Compensatory growth of germline cells has been documented previously in mouse and other organisms (Gilboa and Lehmann, 2006; Lee et al., 2013; Tam and Snow, 1981). As demonstrated in the Drosophila ovary, an equilibrium between germ and soma is maintained partly by feedback from the somatic intermingled cells (ICs), inhibiting the proliferation of PGCs. Mouse gonads might use a similar mechanism. It is also possible that Bmp4 functions in such a compensatory mechanism. Our data suggest that *Msx1* and *Msx2* normally maintain *Bmp4* expression at low level in the ceolomic epithelium, which may be insufficient to support the early entry of PGCs into the cell cycle. In $Msx1^{-/-};Msx2^{-/-}$ mutants, Bmp4 is specifically upregulated in the surface epithelium and possibly gonadal mesoderm of the genital ridge, thus promoting cell cycle entry. It is interesting that in organ culture, Bmp4 induces Kitl expression thus enhancing the survival of PGCs and positively regulating PGC number (Dudley et al., 2007).

Translocation of PGCs from the allantoic mesoderm to the definitive endoderm marks the initiation of their migration. This process was thought to be controlled by the heterotypic repulsive functions of Ifitm1, a member of interferon induced transmembrane family and expressed by cells of mesodermal origin (Tanaka et al., 2010; Tanaka et al., 2005). *Msx1* and *Msx2* function in the mesoderm as PGCs start to migrate. Disrupting *Msx* gene function results in a failure of the incorporation of PGC into the gut endoderm, similar to the phenotype caused by loss of function in *Ifitm1*. Therefore, we hypothesized that *Ifitm1* mediates the control by *Msx1* and *Msx2* of PGC migration. We examined *Ifitm1* expression in $Msx1^{-/-};Msx2^{-/-}$ mutant embryos (Supplementary Fig. 5, finding at both E8.5 and 9.5, *Ifitm1* is upregulated in the dorsal neural tube but slightly downregulated in the paraxial mesoderm in mutant embryos. However, this subtle change of the *Ifitm1* expression pattern does not seem to correlate with the ectopic location of PGCs, suggesting that the pathway by which *Msx1* and *Msx2* regulate PGC migration does not involve *Ifitm1*.

That PGCs migrate through endoderm, and their movement is synchronized with the morphogenesis of the gut is a conserved mechanism that also operates in *Drosophila* and *Caenorhabditis elegans* (Powell-Coffman et al., 1996; Warrior, 1994). The functional role of gut endoderm development in directing murine PGC migration was shown by Hara et al. (2009) in embryos deficient for *Sox17*. Endoderm expansion is arrested in such embryos and a majority of PGCs fail to enter the hindgut at E8.5, moving instead into extraembryonic yolk sac endoderm. It was suggested that PGCs were blocked at the hindgut entrance by clusters of immobile, presumptive endodermal cells marked by E-Cadherin (Hara et al., 2009). No function for *Msx* genes in endoderm development has yet been described. It is unlikely that *Msx* genes play a major role in this process because in $Msx1^{-/-};Msx2^{-/-}$ mutants, gut development is largely unaffected and Cadherin levels are unaltered (Fig. 6F′–I

′). In addition, PGCs are not present in the allantois or yolk sac in significant numbers in the mutants (data not shown).

The migration of PGCs is controlled by a variety of mechanisms, including the chemokine Sdf1/Cxcr4 pathway, signaling between Steel and c-Kit, Wnt5a and Ror2, the cell surface receptor β1-in-tegrin, the cell-cell adhesion molecule E-Cadherin, and the gap junction protein Cx43. Functional roles for each of those molecules/pathways have been demonstrated in loss of function approaches with either knockout or chimeric mouse models (Anderson et al., 1999; Chawengsaksophak et al., 2012; Di Carlo and De Felici, 2000; Francis and Lo, 2006; Gu et al., 2009; Laird et al., 2011; Molyneaux et al., 2003). We showed previously that in the uterus *Msx1, 2* act upstream of *Wnt5a* through a direct interaction with its 5′ *cis*-regulatory sequences (Daikoku et al., 2011). This genetic interaction appears to be stage and tissue-specific: *Msx1*$^{-/-}$;*Msx2*$^{-/-}$ mutant embryos have lower *Wnt5a* mRNA level in the gut mesentery at E9.5 (arrows, Fig. 6D, E) in the gonadal mesoderm at E12.5 (data not shown) but not in the body wall. The PGC migration phenotype in *Msx1*$^{-/-}$;*Msx2*$^{-/-}$ mutants exhibits several characteristics similar to those reported in *Ror2* or *Wnt5a* mutants (Chawengsaksophak et al., 2012; Laird et al., 2011), including ectopic PGC localization in the tail and ectoderm and delayed anterior movement. It is tempting to hypothesize that the decrease in *Wnt5a* expression compromises the ability of PGCs to sense the directional cue from Kitl thus disrupting their migration (Laird et al., 2011). We note, however, that an effect on the *Wnt5a* pathway does not explain how PGCs become trapped in the tail, as levels of *Wnt5a* transcripts are unaltered in this location in mutant embryos.

Glycoproteins of the extracellular matrix (ECM) also play crucial roles in guiding PGC migration (Diez-Torre et al., 2013; Garcia-Castro et al., 1997). Among these, Fibronectin (Fn) is widely expressed throughout the migration route of PGCs, both providing an adhesive substratum and stimulating PGC motility (Alvarez-Buylla and Merchant-Larios, 1986; Ffrench-Constant et al., 1991; Fujimoto et al., 1985). Functional analysis of Fn in PGC migration is hindered by the early embryonic lethality of *Fn*-null mutants (George et al., 1993). Our finding that an upregulation in Fn accompanies the deficiency in PGC migration in *Msx1*$^{-/-}$;*Msx2*$^{-/-}$ mutants suggests that excessive Fn or an enhanced ECM-PGC interaction adversely affects the normal process of PGC homing.

Bmp4 is substantially upregulated in *Msx1*$^{-/-}$;*Msx2*$^{-/-}$ mutant embryos (Fig. 6F–I) (Ishii et al., 2005). Considering its well-documented role in Fn synthesis and assembly (Costello et al., 2009; Molloy et al., 2008; Pegorier et al., 2010; Tang et al., 2003) as well as its ability to stimulate PGC motility in culture (Dudley et al., 2007), we suggest that Bmp4 mediates the effect of *Msx* genes on Fn distribution thus influences PGC migration.

Our observation of tail-localized PGCs in *Msx* mutants resembles a previously described phenotype in *Bax*$^{-/-}$ mutant mice as well as a phenotype in a *mir-290–295*-deficient mutant (Medeiros et al., 2011; Runyan et al., 2008; Runyan et al., 2006; Stallock et al., 2003). If such “tail” PGCs fail to undergo apoptosis, they may develop into extragonadal germ cell tumors (EGCTs). In *Msx1*$^{-/-}$;*Msx2*$^{-/-}$ mutants, we detected apoptosis in some mid-line PGCs (Supplementary Figure 3H), however, the fate of tail PGCs remains unclear. It is

possible that they are protected from apoptosis by increased activity of *Bmp4*, which induces the expression of *Steel factor*, functioning upstream of *Bax* to promote the survival and proliferation of PGCs during their migration (Dudley et al., 2007; Runyan et al., 2006). Therefore, it is important to examine the fate of tail PGCs in *Msx1, 2* mutant embryos at later developmental stages.

Supplementary Material

Refer to Web version on PubMed Central for supplementary material.

Acknowledgments

JS was supported by a training grant from the California Institute of Regenerative Medicine (T1-00004). This work was supported by grants from the NIH to RM (DE012450 and DE016320).

References

Alvarez-Buylla A, Merchant-Larios H. Mouse primordial germ cells use fibronectin as a substrate for migration. Exp Cell Res. 1986; 165:362–368. [PubMed: 3720854]

Anderson R, Copeland TK, Scholer H, Heasman J, Wylie C. The onset of germ cell migration in the mouse embryo. Mech Dev. 2000; 91:61–68. [PubMed: 10704831]

Anderson R, Fassler R, Georges-Labouesse E, Hynes RO, Bader BL, Kreidberg JA, Schaible K, Heasman J, Wylie C. Mouse primordial germ cells lacking beta1 integrins enter the germline but fail to migrate normally to the gonads. Development. 1999; 126:1655–1664. [PubMed: 10079228]

Ara T, Nakamura Y, Egawa T, Sugiyama T, Abe K, Kishimoto T, Matsui Y, Nagasawa T. Impaired colonization of the gonads by primordial germ cells in mice lacking a chemokine, stromal cell-derived factor-1 (SDF-1). Proc Natl Acad Sci USA. 2003; 100:5319–5323. [PubMed: 12684531]

Aramaki S, Hayashi K, Kurimoto K, Ohta H, Yabuta Y, Iwanari H, Mochizuki Y, Hamakubo T, Kato Y, Shirahige K, Saitou M. A mesodermal factor, T, specifies mouse germ cell fate by directly activating germline determinants. Dev Cell. 2013; 27:516–529. [PubMed: 24331926]

Bei M, Maas R. FGFs and BMP4 induce both Msx1-independent and Msx1-dependent signaling pathways in early tooth development. Development. 1998; 125:4325–4333. [PubMed: 9753686]

Bell JR, Noveen A, Liu YH, Ma L, Dobias S, Kundu R, Luo W, Xia Y, Lusis AJ, Snead ML, et al. Genomic structure, chromosomal location, and evolution of the mouse Hox 8 gene. Genomics. 1993; 17:800. [PubMed: 7902329]

Bendel-Stenzel MR, Gomperts M, Anderson R, Heasman J, Wylie C. The role of cadherins during primordial germ cell migration and early gonad formation in the mouse. Mech Dev. 2000; 91:143–152. [PubMed: 10704839]

Brugger SM, Merrill AE, Torres-Vazquez J, Wu N, Ting MC, Cho JY, Dobias SL, Yi SE, Lyons K, Bell JR, Arora K, Warrior R, Maxson R. A phylogenetically conserved cis-regulatory module in the Msx2 promoter is sufficient for BMP-dependent transcription in murine and Drosophila embryos. Development. 2004; 131:5153–5165. [PubMed: 15459107]

Chawengsaksophak K, Svingen T, Ng ET, Epp T, Spiller CM, Clark C, Cooper H, Koopman P. Loss of Wnt5a disrupts primordial germ cell migration and male sexual development in mice. Biol Reprod. 2012; 86:1–12.

Chen YH, Ishii M, Sun J, Sucov HM, Maxson RE Jr. Msx1 and Msx2 regulate survival of secondary heart field precursors and post-migratory proliferation of cardiac neural crest in the outflow tract. Dev Biol. 2007; 308:421–437. [PubMed: 17601530]

Chuva de Sousa Lopes SM, van den Driesche S, Carvalho RL, Larsson J, Eggen B, Surani MA, Mummery CL. Altered primordial germ cell migration in the absence of transforming growth factor beta signaling via ALK5. Dev Biol. 2005; 284:194–203. [PubMed: 15993878]

Costello I, Biondi CA, Taylor JM, Bikoff EK, Robertson EJ. Smad4-dependent pathways control basement membrane deposition and endodermal cell migration at early stages of mouse development. BMC Dev Biol. 2009; 9:54. [PubMed: 19849841]

Daikoku T, Cha J, Sun X, Tranguch S, Xie H, Fujita T, Hirota Y, Lydon J, De-Mayo F, Maxson R, Dey SK. Conditional deletion of Msx homeobox genes in the uterus inhibits blastocyst implantation by altering uterine receptivity. Dev Cell. 2011; 21:1014–1025. [PubMed: 22100262]

De Felici M, Dolci S. In vitro adhesion of mouse fetal germ cells to extracellular matrix components. Cell Differ Dev. 1989; 26:87–96. [PubMed: 2706569]

De Felici M, Dolci S, Pesce M. Cellular and molecular aspects of mouse primordial germ cell migration and proliferation in culture. Int J Dev Biol. 1992; 36:205–213. [PubMed: 1381942]

Di Carlo A, De Felici M. A role for E-cadherin in mouse primordial germ cell development. Dev Biol. 2000; 226:209–219. [PubMed: 11023681]

Diez-Torre A, Diaz-Nunez M, Eguizabal C, Silvan U, Arechaga J. Evidence for a role of matrix metalloproteinases and their inhibitors in primordial germ cell migration. Andrology. 2013; 1:779–786. [PubMed: 23843195]

Dudley BM, Runyan C, Takeuchi Y, Schaible K, Molyneaux K. BMP signaling regulates PGC numbers and motility in organ culture. Mech Dev. 2007; 124:68–77. [PubMed: 17112707]

Ffrench-Constant C, Hollingsworth A, Heasman J, Wylie CC. Response to fibronectin of mouse primordial germ cells before, during and after migration. Development. 1991; 113:1365–1373. [PubMed: 1688357]

Francis RJ, Lo CW. Primordial germ cell deficiency in the connexin 43 knockout mouse arises from apoptosis associated with abnormal p53 activation. Development. 2006; 133:3451–3460. [PubMed: 16887824]

Fu H, Ishii M, Gu Y, Maxson R. Conditional alleles of Msx1 and Msx2. Genesis. 2007; 45:477–481. [PubMed: 17654563]

Fujimoto T, Yoshinaga K, Kono I. Distribution of fibronectin on the migratory pathway of primordial germ cells in mice. Anat Rec. 1985; 211:271–278. [PubMed: 3993980]

Furuta Y, Hogan BL. BMP4 is essential for lens induction in the mouse embryo. Genes Dev. 1998; 12:3764–3775. [PubMed: 9851982]

Garcia-Castro MI, Anderson R, Heasman J, Wylie C. Interactions between germ cells and extracellular matrix glycoproteins during migration and gonad assembly in the mouse embryo. J Cell Biol. 1997; 138:471–480. [PubMed: 9230086]

Gauchat D, Mazet F, Berney C, Schummer M, Kreger S, Pawlowski J, Galliot B. Evolution of Antp-class genes and differential expression of Hydra Hox/paraHox genes in anterior patterning. Proc Natl Acad Sci USA. 2000; 97:4493–4498. [PubMed: 10781050]

George EL, Georges-Labouesse EN, Patel-King RS, Rayburn H, Hynes RO. Defects in mesoderm, neural tube and vascular development in mouse embryos lacking fibronectin. Development. 1993; 119:1079–1091. [PubMed: 8306876]

Gilboa L, Lehmann R. Soma-germline interactions coordinate homeostasis and growth in the Drosophila gonad. Nature. 2006; 443:97–100. [PubMed: 16936717]

Ginsburg M, Snow MH, McLaren A. Primordial germ cells in the mouse embryo during gastrulation. Development. 1990; 110:521–528. [PubMed: 2133553]

Gu Y, Runyan C, Shoemaker A, Surani A, Wylie C. Steel factor controls primordial germ cell survival and motility from the time of their specification in the allantois, and provides a continuous niche throughout their migration. Development. 2009; 136:1295–1303. [PubMed: 19279135]

Han J, Ishii M, Bringas P Jr, Maas RL, Maxson RE Jr, Chai Y. Concerted action of Msx1 and Msx2 in regulating cranial neural crest cell differentiation during frontal bone development. Mech Dev. 2007; 124:729–745. [PubMed: 17693062]

Hara K, Kanai-Azuma M, Uemura M, Shitara H, Taya C, Yonekawa H, Kawakami H, Tsunekawa N, Kurohmaru M, Kanai Y. Evidence for crucial role of hindgut expansion in directing proper migration of primordial germ cells in mouse early embryogenesis. Dev Biol. 2009; 330:427–439. [PubMed: 19371732]

Hogan, B., Beddington, R., Costantini, F., Lacy, E. Manipulating the Mouse Embryo: A Laboratory Manual. Cold Spring Harbor Press; New York: 1994.

Huang WW, Yin Y, Bi Q, Chiang TC, Garner N, Vuoristo J, McLachlan JA, Ma L. Developmental diethylstilbestrol exposure alters genetic pathways of uterine cytodifferentiation. Mol Endocrinol. 2005; 19:669–682. [PubMed: 15591538]

Hussein SM, Duff EK, Sirard C. Smad4 and beta-catenin co-activators functionally interact with lymphoid-enhancing factor to regulate graded expression of Msx2. J Biol Chem. 2003; 278:48805–48814. [PubMed: 14551209]

Iler N, Abate-Shen C. Rapid identification of homeodomain binding sites in the Wnt-5a gene using an immunoprecipitation strategy. Biochem Biophys Res Commun. 1996; 227:257–265. [PubMed: 8858134]

Ishii M, Han J, Yen HY, Sucov HM, Chai Y, Maxson RE Jr. Combined deficiencies of Msx1 and Msx2 cause impaired patterning and survival of the cranial neural crest. Development. 2005; 132:4937–4950. [PubMed: 16221730]

Ishii M, Merrill AE, Chan YS, Gitelman I, Rice DP, Sucov HM, Maxson RE Jr. Msx2 and Twist cooperatively control the development of the neural crest-derived skeletogenic mesenchyme of the murine skull vault. Development. 2003; 130:6131–6142. [PubMed: 14597577]

Kurimoto K, Yabuta Y, Ohinata Y, Shigeta M, Yamanaka K, Saitou M. Complex genome-wide transcription dynamics orchestrated by Blimp1 for the specification of the germ cell lineage in mice. Genes Dev. 2008; 22:1617–1635. [PubMed: 18559478]

Laird DJ, Altshuler-Keylin S, Kissner MD, Zhou X, Anderson KV. Ror2 enhances polarity and directional migration of primordial germ cells. PLoS Genet. 2011; 7:e1002428. [PubMed: 22216013]

Lallemand Y, Nicola MA, Ramos C, Bach A, Clement CS, Robert B. Analysis of Msx1; Msx2 double mutants reveals multiple roles for Msx genes in limb development. Development. 2005; 132:3003–3014. [PubMed: 15930102]

Lawson KA, Dunn NR, Roelen BA, Zeinstra LM, Davis AM, Wright CV, Korving JP, Hogan BL. Bmp4 is required for the generation of primordial germ cells in the mouse embryo. Genes Dev. 1999; 13:424–436. [PubMed: 10049358]

Le Bouffant R, Souquet B, Duval N, Duquenne C, Herve R, Frydman N, Robert B, Habert R, Livera G. Msx1 and Msx2 promote meiosis initiation. Development. 2011; 138:5393–5402. [PubMed: 22071108]

Lee H, Kim S, Park T, Rengaraj D, Park K, Lee H, Park SB, Kim S, Choi SB, Han J. Compensatory proliferation of endogenous chicken primordial germ cells after elimination by busulfan treatment. Stem Cell Res Ther. 2013; 4:136. [PubMed: 24405696]

Magnusdottir E, Dietmann S, Murakami K, Gunesdogan U, Tang F, Bao S, Diamanti E, Lao K, Gottgens B, Azim Surani M. A tripartite transcription factor network regulates primordial germ cell specification in mice. Nat Cell Biol. 2013; 15:905–915. [PubMed: 23851488]

Marazzi G, Wang Y, Sassoon D. Msx2 is a transcriptional regulator in the BMP4-mediated programmed cell death pathway. Dev Biol. 1997; 186:127–138. [PubMed: 9205134]

Medeiros LA, Dennis LM, Gill ME, Houbaviy H, Markoulaki S, Fu D, White AC, Kirak O, Sharp PA, Page DC, Jaenisch R. Mir-290-295 deficiency in mice results in partially penetrant embryonic lethality and germ cell defects. Proc Natl Acad Sci USA. 2011; 108:14163–14168. [PubMed: 21844366]

Molloy EL, Adams A, Moore JB, Masterson JC, Madrigal-Estebas L, Mahon BP, O'Dea S. BMP4 induces an epithelial-mesenchymal transition-like response in adult airway epithelial cells. Growth Factors. 2008; 26:12–22. [PubMed: 18365875]

Molyneaux K, Wylie C. Primordial germ cell migration. Int J Dev Biol. 2004; 48:537–544. [PubMed: 15349828]

Molyneaux KA, Stallock J, Schaible K, Wylie C. Time-lapse analysis of living mouse germ cell migration. Dev Biol. 2001; 240:488–498. [PubMed: 11784078]

Molyneaux KA, Zinszner H, Kunwar PS, Schaible K, Stebler J, Sunshine MJ, O'Brien W, Raz E, Littman D, Wylie C, Lehmann R. The chemokine SDF1/CXCL12 and its receptor CXCR4 regulate mouse germ cell migration and survival. Development. 2003; 130:4279–4286. [PubMed: 12900445]

Nakaki F, Hayashi K, Ohta H, Kurimoto K, Yabuta Y, Saitou M. Induction of mouse germ-cell fate by transcription factors in vitro. Nature. 2013; 501:222–226. [PubMed: 23913270]

Ohinata Y, Ohta H, Shigeta M, Yamanaka K, Wakayama T, Saitou M. A signaling principle for the specification of the germ cell lineage in mice. Cell. 2009; 137:571–584. [PubMed: 19410550]

Ohinata Y, Payer B, O'Carroll D, Ancelin K, Ono Y, Sano M, Barton SC, Obukhanych T, Nussenzweig M, Tarakhovsky A, Saitou M, Surani MA. Blimp1 is a critical determinant of the germ cell lineage in mice. Nature. 2005; 436:207–213. [PubMed: 15937476]

Pegorier S, Campbell GA, Kay AB, Lloyd CM. Bone morphogenetic protein (BMP)-4 and BMP-7 regulate differentially transforming growth factor (TGF)-beta1 in normal human lung fibroblasts (NHLF). Respir Res. 2010; 11:85. [PubMed: 20573231]

Phippard DJ, Weber-Hall SJ, Sharpe PT, Naylor MS, Jayatalake H, Maas R, Woo I, Roberts-Clark D, Francis-West PH, Liu YH, Maxson R, Hill RE, Dale TC. Regulation of Msx-1, Msx-2, Bmp-2 and Bmp-4 during foetal and postnatal mammary gland development. Development. 1996; 122:2729–2737. [PubMed: 8787747]

Pollard SL, Holland PW. Evidence for 14 homeobox gene clusters in human genome ancestry. Curr Biol. 2000; 10:1059–1062. [PubMed: 10996074]

Powell-Coffman JA, Knight J, Wood WB. Onset of *C. elegans* gastrulation is blocked by inhibition of embryonic transcription with an RNA polymerase antisense RNA. Dev Biol. 1996; 178:472–483. [PubMed: 8812143]

Richardson BE, Lehmann R. Mechanisms guiding primordial germ cell migration: strategies from different organisms. Nat Rev Mol Cell Biol. 2010; 11:37–49. [PubMed: 20027186]

Roybal PG, Wu NL, Sun J, Ting MC, Schafer CA, Maxson RE. Inactivation of Msx1 and Msx2 in neural crest reveals an unexpected role in suppressing heterotopic bone formation in the head. Dev Biol. 2010; 343:28–39. [PubMed: 20398647]

Runyan C, Gu Y, Shoemaker A, Looijenga L, Wylie C. The distribution and behavior of extragonadal primordial germ cells in Bax mutant mice suggest a novel origin for sacrococcygeal germ cell tumors. Int J Dev Biol. 2008; 52:333–344. [PubMed: 18415933]

Runyan C, Schaible K, Molyneaux K, Wang Z, Levin L, Wylie C. Steel factor controls midline cell death of primordial germ cells and is essential for their normal proliferation and migration. Development. 2006; 133:4861–4869. [PubMed: 17107997]

Saga Y, Hata N, Kobayashi S, Magnuson T, Seldin MF, Taketo MM. MesP1: a novel basic helix-loop-helix protein expressed in the nascent mesodermal cells during mouse gastrulation. Development. 1996; 122:2769–2778. [PubMed: 8787751]

Saga Y, Miyagawa-Tomita S, Takagi A, Kitajima S, Miyazaki J, Inoue T. MesP1 is expressed in the heart precursor cells and required for the formation of a single heart tube. Development. 1999; 126:3437–3447. [PubMed: 10393122]

Saitou M, Barton SC, Surani MA. A molecular programme for the specification of germ cell fate in mice. Nature. 2002; 418:293–300. [PubMed: 12124616]

Satokata I, Maas R. Msx1 deficient mice exhibit cleft palate and abnormalities of craniofacial and tooth development. Nat Genet. 1994; 6:348–356. [PubMed: 7914451]

Satokata I, Ma L, Ohshima H, Bei M, Woo I, Nishizawa K, Maeda T, Takano Y, Uchiyama M, Heaney S, Peters H, Tang Z, Maxson R, Maas R. Msx2 deficiency in mice causes pleiotropic defects in bone growth and ectodermal organ formation. Nat Genet. 2000; 24:391–395. [PubMed: 10742104]

Soriano P. Generalized lacZ expression with the ROSA26 Cre reporter strain. Nat Genet. 1999; 21:70–71. [PubMed: 9916792]

Stallock J, Molyneaux K, Schaible K, Knudson CM, Wylie C. The pro-apoptotic gene Bax is required for the death of ectopic primordial germ cells during their migration in the mouse embryo. Development. 2003; 130:6589–6597. [PubMed: 14660547]

Sun J, Ishii M, Ting MC, Maxson R. Foxc1 controls the growth of the murine frontal bone rudiment by direct regulation of a Bmp response threshold of Msx2. Development. 2013; 140:1034–1044. [PubMed: 23344708]

Tam PP, Snow MH. Proliferation and migration of primordial germ cells during compensatory growth in mouse embryos. J Embryol Exp Morphol. 1981; 64:133–147. [PubMed: 7310300]

Tanaka SS, Yamaguchi YL, Tsoi B, Lickert H, Tam PP. IFITM/Mil/fragilis family proteins IFITM1 and IFITM3 play distinct roles in mouse primordial germ cell homing and repulsion. Dev Cell. 2005; 9:745–756. [PubMed: 16326387]

Tanaka SS, Yamaguchi YL, Steiner KA, Nakano T, Nishinakamura R, Kwan KM, Behringer RR, Tam PP. Loss of Lhx1 activity impacts on the localization of primordial germ cells in the mouse. Dev Dyn. 2010; 239:2851–2859. [PubMed: 20845430]

Tang CH, Yang RS, Liou HC, Fu WM. Enhancement of fibronectin synthesis and fibrillogenesis by BMP-4 in cultured rat osteoblast. J Bone Miner Res. 2003; 18:502–511. [PubMed: 12619935]

Ting MC, Wu NL, Roybal PG, Sun J, Liu L, Yen Y, Maxson RE Jr. EphA4 as an effector of Twist1 in the guidance of osteogenic precursor cells during calvarial bone growth and in craniosynostosis. Development. 2009; 136:855–864. [PubMed: 19201948]

Vainio S, Karavanova I, Jowett A, Thesleff I. Identification of BMP-4 as a signal mediating secondary induction between epithelial and mesenchymal tissues during early tooth development. Cell. 1993; 75:45–58. [PubMed: 8104708]

Warrior R. Primordial germ cell migration and the assembly of the Drosophila embryonic gonad. Dev Biol. 1994; 166:180–194. [PubMed: 7958445]

Willert J, Epping M, Pollack JR, Brown PO, Nusse R. A transcriptional response to Wnt protein in human embryonic carcinoma cells. BMC Dev Biol. 2002; 2:8. [PubMed: 12095419]

Yamaji M, Seki Y, Kurimoto K, Yabuta Y, Yuasa M, Shigeta M, Yamanaka K, Ohinata Y, Saitou M. Critical function of Prdm14 for the establishment of the germ cell lineage in mice. Nat Genet. 2008; 40:1016–1022. [PubMed: 18622394]

Ying Y, Zhao GQ. Cooperation of endoderm-derived BMP2 and extra-embryonic ectoderm-derived BMP4 in primordial germ cell generation in the mouse. Dev Biol. 2001; 232:484–492. [PubMed: 11401407]

Ying Y, Qi X, Zhao GQ. Induction of primordial germ cells from murine epiblasts by synergistic action of BMP4 and BMP8B signaling pathways. Proc Natl Acad Sci USA. 2001; 98:7858–7862. [PubMed: 11427739]

Ying Y, Liu XM, Marble A, Lawson KA, Zhao GQ. Requirement of Bmp8b for the generation of primordial germ cells in the mouse. Mol Endocrinol. 2000; 14:1053–1063. [PubMed: 10894154]

Appendix A. Supplementary material

Supplementary data associated with this article can be found in the online version at http://dx.doi.org/10.1016/j.ydbio.2016.07.013.

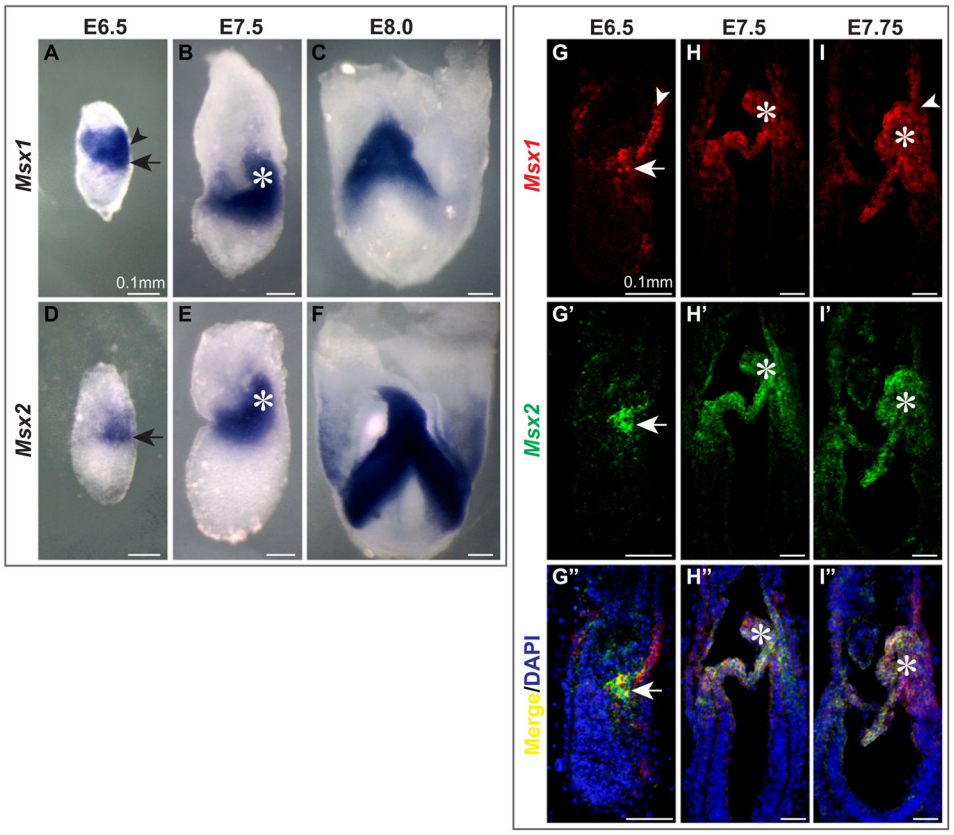

Fig. 1.

Msx1 and *Msx2* are expressed in tissues from which PGCs arise. We performed whole mount (A–F) and section (G–I″) *in situ* hybridization with RNA probes against *Msx1* and *Msx2* on wild-type embryos from E6.5 to E8.0. Sagittal sections were subjected to *in situ* hybridization with *Msx1* (red) and *Msx2* (green) probes simultaneously and signals were amplified by TSA (TSA™PLUS, Perkin Elmer). (A, D, G–G″) *Msx1* transcripts were present in visceral endoderm (arrowhead) and the posterior end of the primitive streak (arrow), while *Msx2* transcripts were located mainly in the nascent mesoderm (arrow). (B, E, H–H″, I–I″) *Msx1* and *Msx2* were both strongly expressed in the mesoderm including the allantois (asterisks). (C, F) Allantoic bud and embryonic mesoderm expressed *Msx* genes with high intensity.

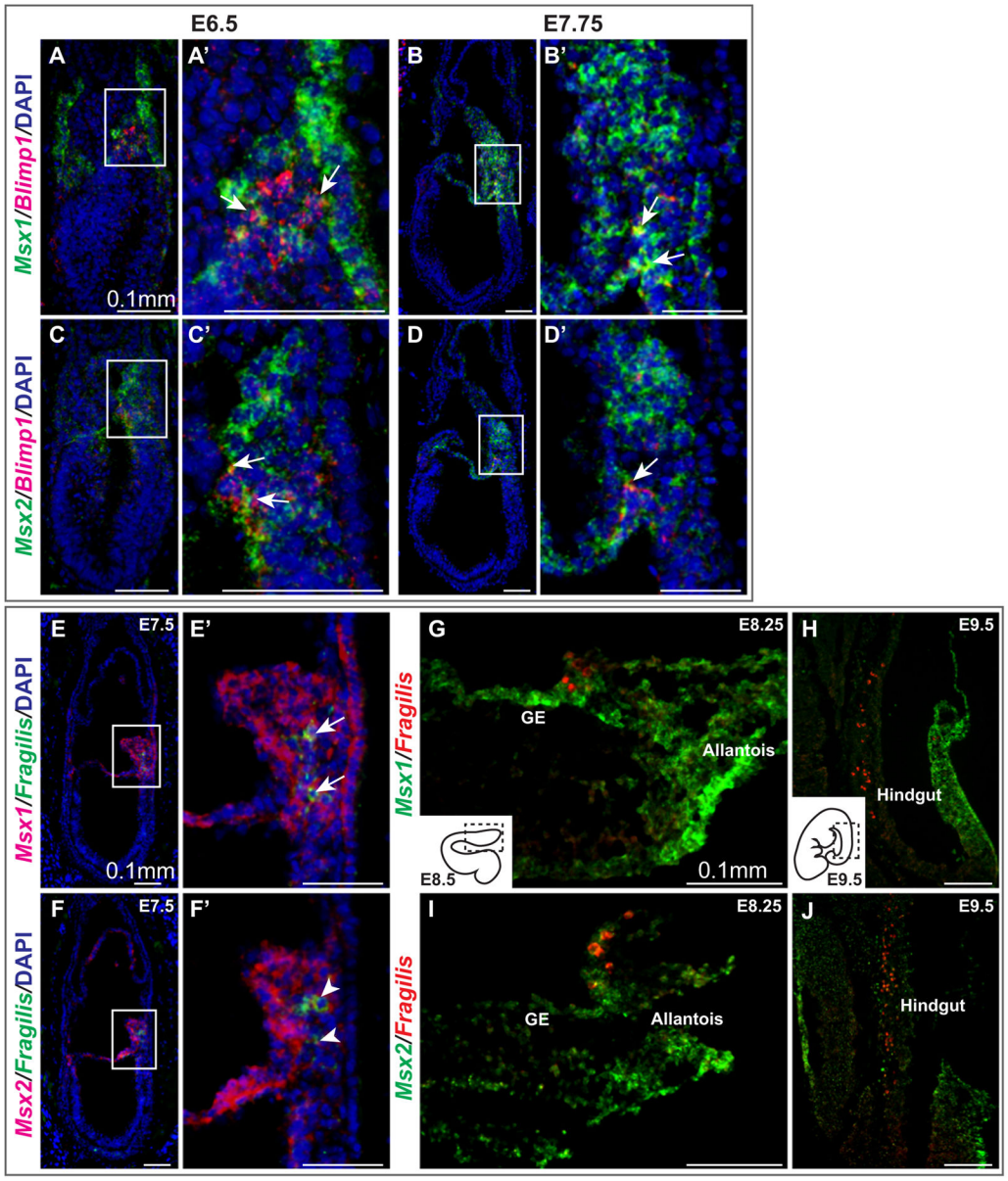

Fig. 2.

Transient expression of *Msx1* and *Msx2* in the germline during the specification of PGCs. (A–D′) Sagittal sections from E6.5 and E7.5 wild-type embryos were collected and subjected to *in situ* hybridization with RNA probes against *Msx1* or *Msx2* (green) and *Blimp1* (red) simultaneously. Immunofluorescence was used for detection. With both *Msx1* and *Msx2*, some overlap with *Blimp1* was evident (arrows), suggesting that a subpopulation of PGC precursors expresses *Msx* genes. (E–F′) A *Fragilis* RNA probe (green) was used with *Msx1* or *Msx2* (red) to confirm this result. (G–J) *Msx1* was expressed in allantois, visceral endoderm and gut endoderm (GE) where PGCs are found at approximately E8.25. *Msx2* was expressed in the allantois. By E9.5, when PGCs migrate up along the hindgut, *Msx1* and *Msx2* were expressed in the body wall.

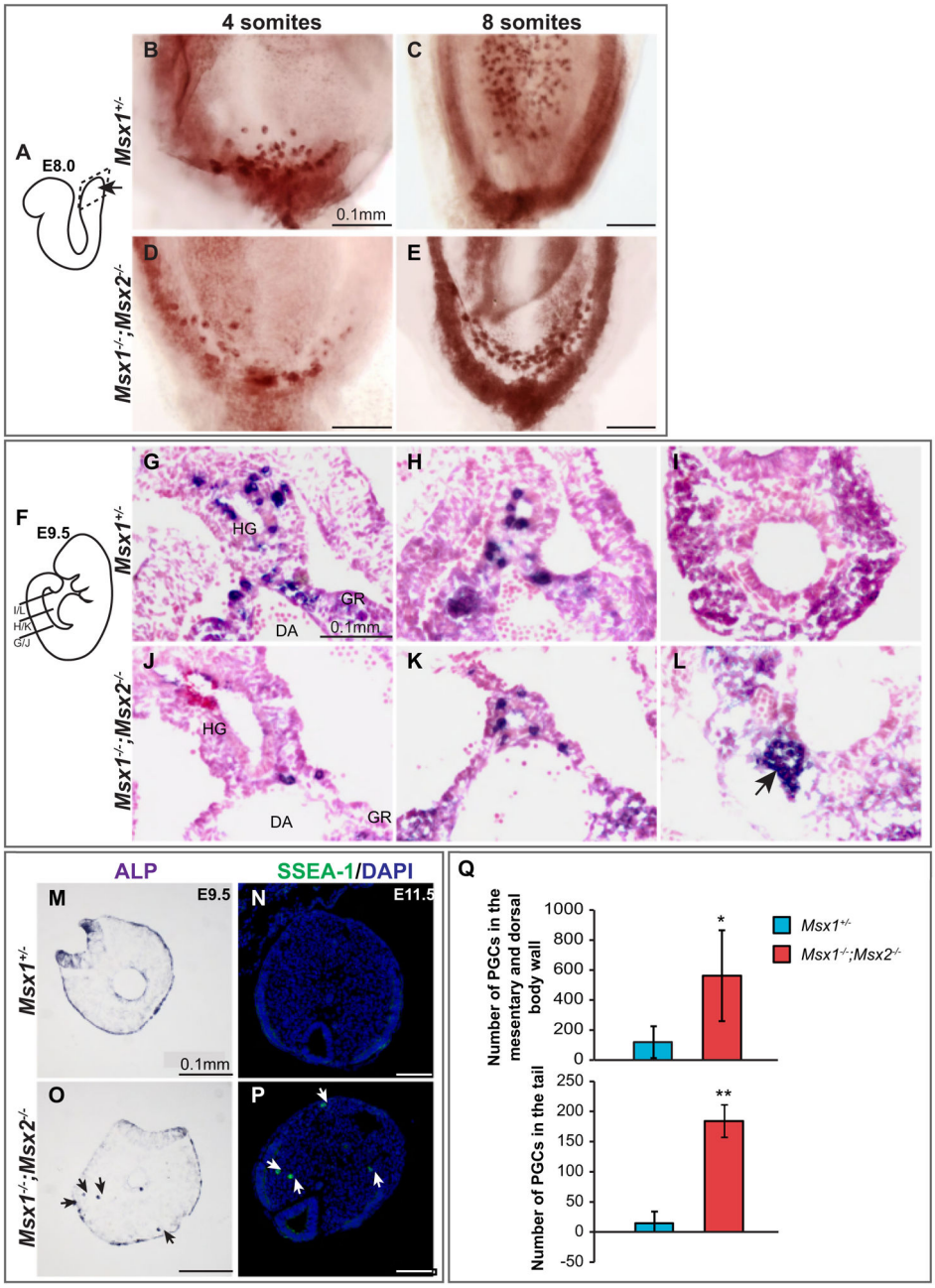

Fig. 3.

Altered PGC migration in *Msx1*$^{-/-}$;*Msx2*$^{-/-}$ mutant embryos. (A–E) E8.0 embryos were harvested and subjected to whole mount alkaline phosphatase staining to visualize PGCs. Images show a ventral view of the caudal region as indicated in (A). Distribution of PGCs in the gut endoderm was less confined in *Msx1*$^{-/-}$;*Msx2*$^{-/-}$ mutants (C, E) compared to *Msx1*$^{+/-}$ controls (B, D). (F–L) For E9.5 embryos, ALP staining was performed after frozen sectioning to compare the distribution of PGCs along the A–P axis. (F) Transverse sections were cut through the hindgut and are shown here from anterior to posterior. (G–I) In *Msx1*$^{+/-}$ controls, more PGCs were found in the anterior hindgut mesentery and no PGCs

were left in the tail region. (J–L) In *Msx1*$^{-/-}$;*Msx2*$^{-/-}$ mutants, fewer PGCs had reached the anterior hindgut, while a large cluster of PGCs was found around the posterior end of the hindgut in the tail. HG, hindgut; GR, genital ridge; DA, dorsal aorta. (M–P) Ectopic PGCs found in the tail and epithelium are not incorporated into the hindgut (arrows). (Q) Posterior portions from three pairs of *Msx1*$^{+/-}$ controls and *Msx1*$^{-/-}$;*Msx2*$^{-/-}$ mutants at E12.5 were sectioned and stained for ALP to count PGCs. PGC migration in the mutants was greatly delayed, as indicated by a significant increase in the number of PGCs localized in the mesentery and dorsal body wall. (asterisk, $P<0.1$). Significantly more tail PGCs were found in the mutants (double asterisks, $P<0.001$).

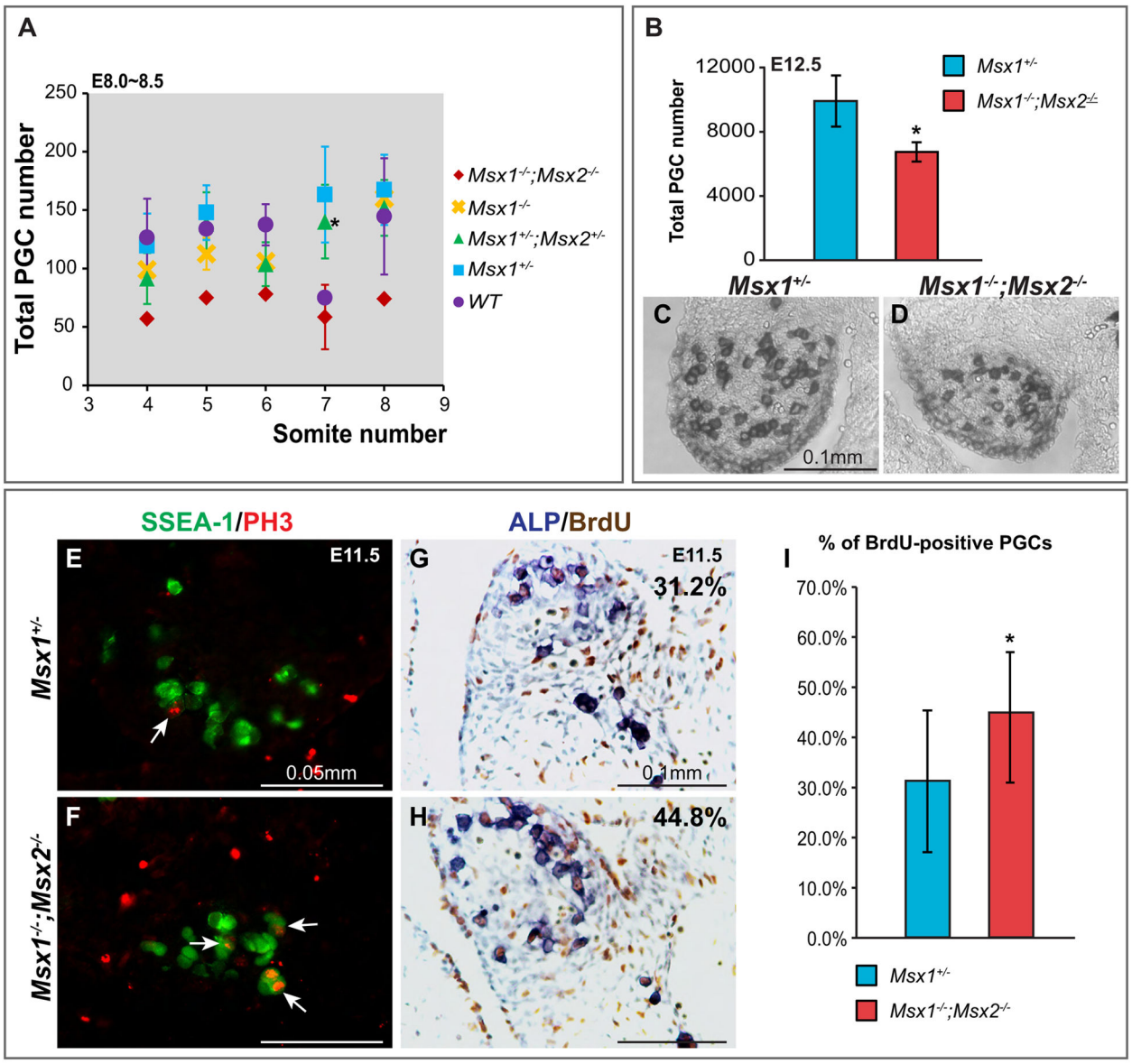

Fig. 4.

Reduced number of PGCs in *Msx1*$^{-/-}$;*Msx2*$^{-/-}$ mutant embryos. (A) PGC numbers counted from E8.0–8.5 embryos were plotted relative to somite number. If more than one embryo of the same somite number was harvested, the average and standard deviation was calculated. *Msx1*$^{-/-}$;*Msx2*$^{-/-}$ mutants contain fewer PGCs compared to the embryos of other genotypes. At the 7-somite stage, significance (asterisk, P<0.05) was obtained when comparing *Msx1*$^{-/-}$;*Msx2*$^{-/-}$ to *Msx1*$^{+/-}$;*Msx2*$^{+/-}$ embryos. (B–D) Transverse sections from E12.5 *Msx1*$^{-/-}$;*Msx2*$^{-/-}$ mutants and *Msx1*$^{+/-}$ controls (n=3 for both genotypes) were stained for ALP to identify PGCs. The genital ridge in the mutants is smaller in size and contains visibly fewer PGCs (D). The total number of PGCs is significantly lower in *Msx1*$^{-/-}$;*Msx2*$^{-/-}$ mutant (asterisk, P<0.05, B). (E–F) Proliferating PGCs in S phase were identified by incubating sections of E11.5 mutant and control embryos with an SSEA-1 antibody (in green) and a PH3 antibody (in red) simultaneously (arrows). (G–I) Sections

from E11.5 embryos were also double stained for BrdU and ALP to calculate the percentage of dividing PGCs. The BrdU incorporation rate in *Msx1*$^{-/-}$;*Msx2*$^{-/-}$ mutants (44.8%) is slightly but significantly higher than it in *Msx1*$^{+/-}$ controls (31.2%) (asterisk, P<0.001, I). Two pairs of BrdU/ALP double stained embryos were compared, data shown is from one pair but representative of both.

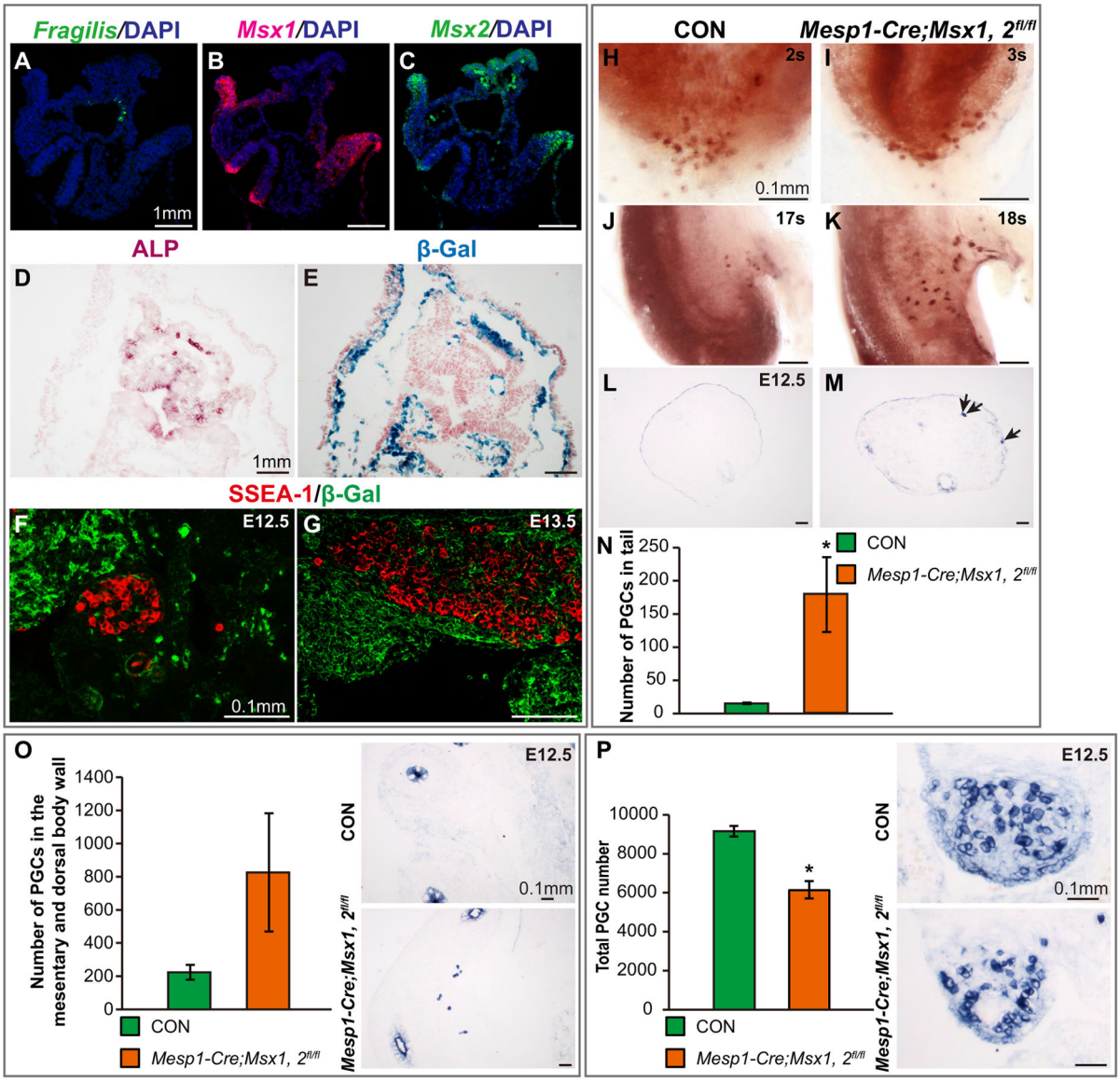

Fig. 5.

Mesp1-Cre;Msx1, $2^{fl/fl}$ mutant embryos exhibit a PGC phenotype similar to conventional *Msx1, 2* mutants. (A–C) Transverse sections across the caudal region of E8.5 embryos were subjected to *in situ* hybridization with probes against *Fragilis* (A), *Msx1* (B) and *Msx2* (C). *Fragilis* marks PGCs embedded in the gut epithelium. *Msx1* and *Msx2* are expressed most intensely in somatic mesoderm and the most dorsal part of the neural tube. Transcripts of *Msx1* and *Msx2* were also detected in the visceral mesoderm. (D and E) *Mesp1-Cre;R26R*$^{LacZ/LacZ}$ embryos were harvested at E8.5 and prepared for frozen sectioning. Comparable sections were stained in parallel for ALP to identify PGCs and β-Gal to mark the Cre activity respectively. PGCs are embedded in the gut epithelium (D), while *lacZ* staining was seen in the mesoderm surrounding the gut (E). (F, G) A mouse SSEA-1 antibody (in red) and a rabbit β-Gal antibody (in green) were used to stain PGCs and Cre activity simultaneously. No PGCs were found to express β-Gal. (H–K) E8.0 to E9.0 *Mesp1-*

Cre;Msx1,2$^{fl/fl}$ mutants and controls were subjected to whole mount ALP staining. At E8.0, PGCs in the mutants are spread laterally around the caudal end of the embryos (I) whereas in the controls, PGCs are more confined to the midline (H). More tail-localized PGCs (K) were observed in the mutants at E9.0 when majority of PGCs have already migrated up (J′, K′). (L–P) Transverse sections from E12.5 *Mesp1-Cre;Msx1,2*$^{fl/fl}$ mutants (n=3) and controls (*Mesp1-Cre* negative littermates, n=3) were stained for ALP to identify PGCs. Numbers of PGCs in different locations were counted. Significantly more tail PGCs (arrows, M) were found in the mutants (asterisk, $P<0.05$, N). (O) In *Mesp1-Cre;Msx1,2*$^{fl/fl}$ mutants, more PGCs in the mesentery and dorsal body wall indicated a substantial delay in PGC migration. (P) the Size of the gonad and the total number of PGCs were reduced in *Mesp1-Cre;Msx1,2*$^{fl/fl}$ mutants (asterisk, $P<0.001$).

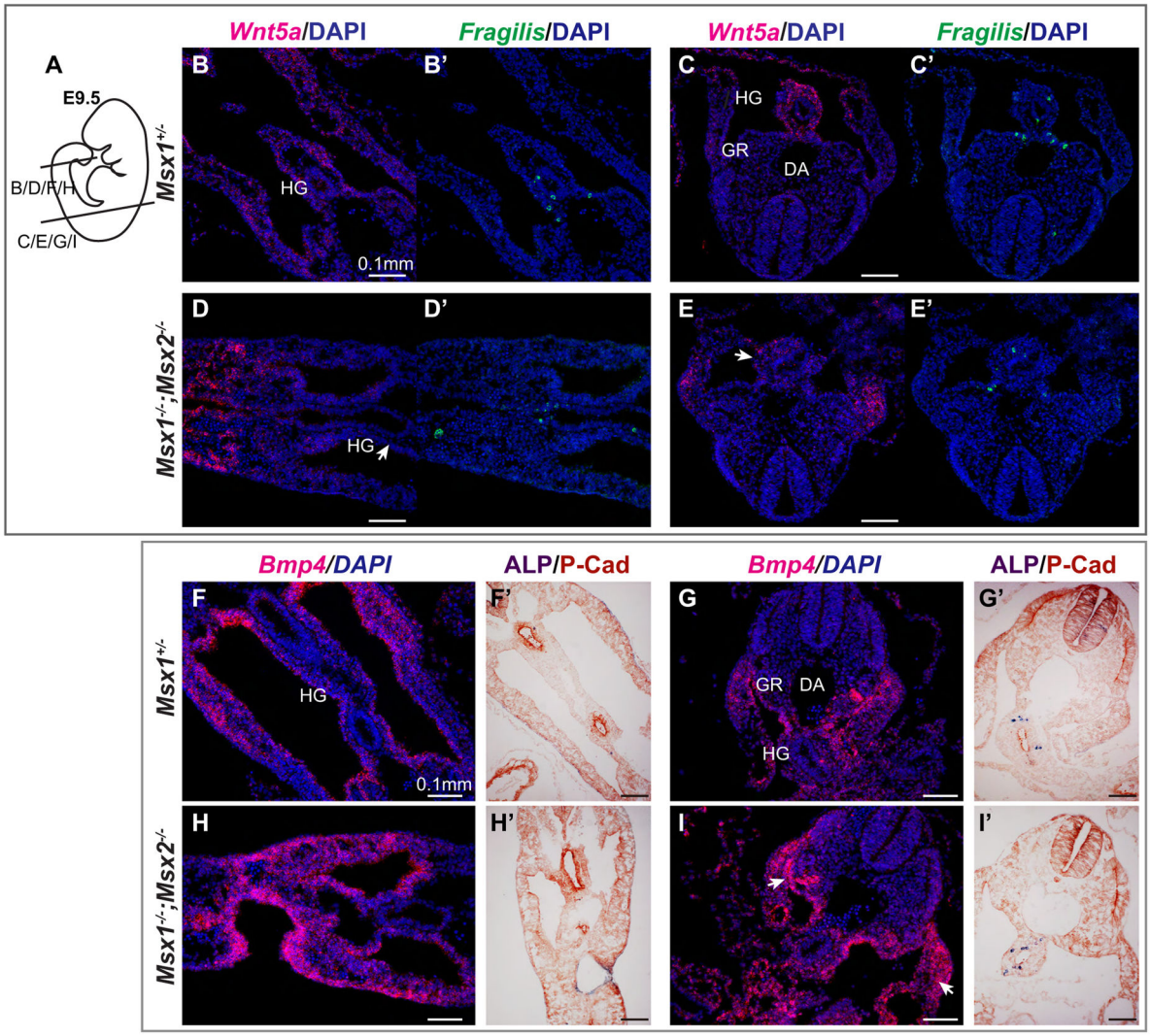

Fig. 6.

Msx1$^{-/-}$;*Msx2*$^{-/-}$ mutant embryos exhibit a decrease in *Wnt5a* mRNA in the hindgut mesentery and an increase in *Bmp4* mRNA in the surface epithelium of the gonad. (A–E′) E9.5 embryos were sectioned and subjected to *in situ* hybridization with a *Wnt5a* RNA probe (in red, B–E) and a *Fragilis* probe (in green, B′–E′) simultaneously. Images shown are transverse sections from posterior (B, B′, D, D′) to anterior (C, C′, E, E′) as in (A). Note the reduced *Wnt5a* signal in the mesoderm around the gut in *Msx1*$^{-/-}$;*Msx2*$^{-/-}$ mutants (arrows, D, E) compared to *Msx1*$^{+/-}$ controls (B, C). Section *in situ* hybridization was also performed with a *Bmp4* probe at E9.5 (F–I). Adjacent sections were incubated with an anti-Pan-Cadherin antibody following ALP staining to mark the location of PGCs (F′–I′). More concentrated *Bmp4* transcripts were observed in the ceolomic epithelium as well as the body wall (arrows, I). HG, hindgut; GR, genital ridge; DA, dorsal aorta.

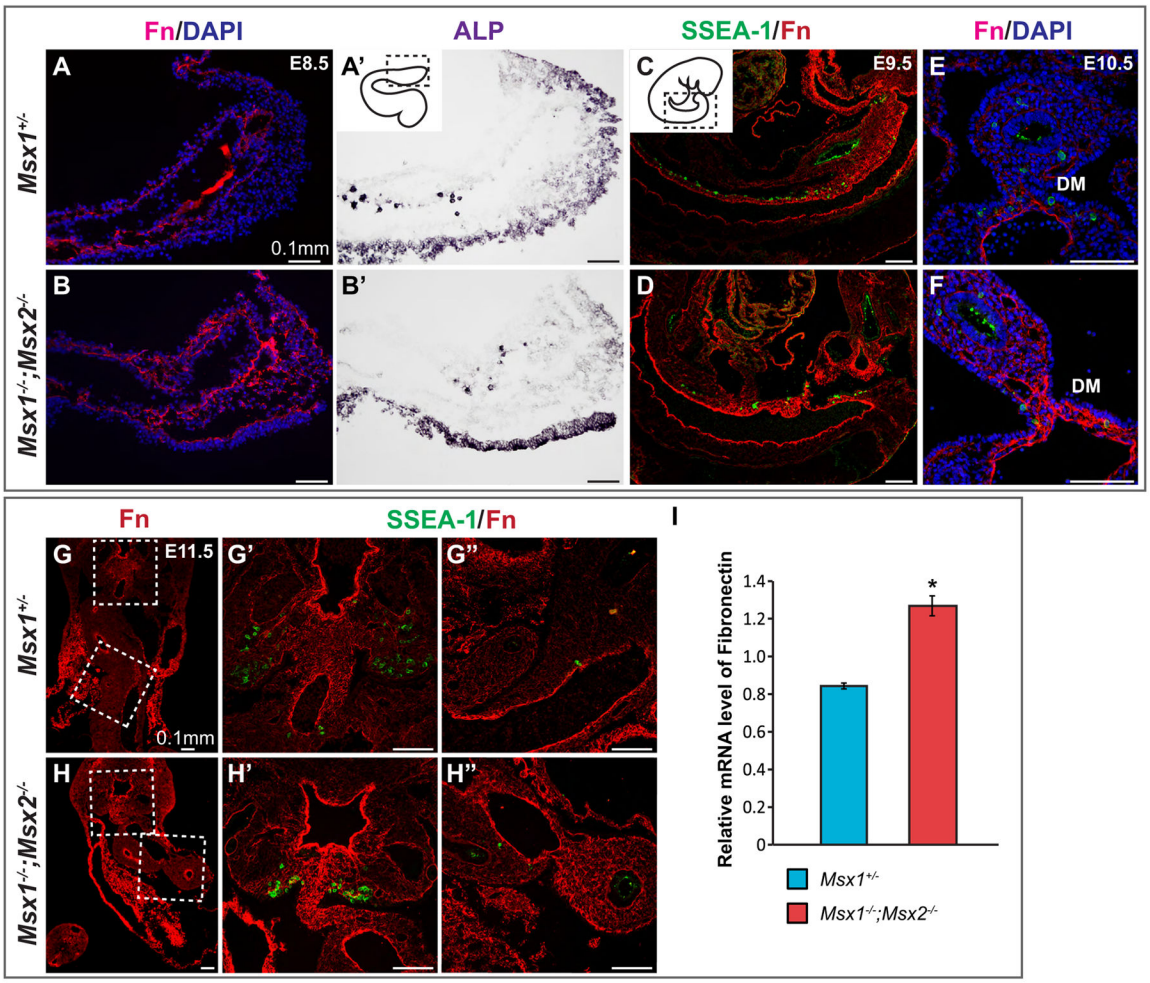

Fig. 7.

Upregulation of Fibronectin in *Msx1*$^{-/-}$;*Msx2*$^{-/-}$ mutant embryos. (A–D) Sagittal sections were collected from E8.5 to E9.5 *Msx1*$^{-/-}$;*Msx2*$^{-/-}$ mutant embryos and controls. Immunostaining with an anti-Fibronectin antibody (in red) was carried out in parallel with ALP staining (A′, B′) for E8.5 embryos and simultaneously with a SSEA-1 antibody (in green, C, D) for E9.5 embryos. An upregulation of Fibronectin was detected in the basal lamina (arrow, B) and the mesentery around the gut endoderm (arrow, D) in *Msx1*$^{-/-}$;*Msx2*$^{-/-}$ mutants. (E, F) Transverse sections from E10.5 mutant and control embryos were stained with Fibronectin and SSEA-1 antibodies simultaneously. Note the narrow and elongated dorsal mesentery in the mutant and its highly concentrated Fn that was in direct contact with PGCs (arrows, F). (G–H″) Transverse sections were collected in parallel from E11.5 mutant and control embryos. One set of the sections was subjected to *in situ* hybridization with an *Fn* ribonucleotide probe (in red, G, H), while another set was stained with Fibronectin and SSEA-1 antibodies (G′-H″). G′ and G″, showing the dorsal mesentery and hindgut mesentery respectively, correspond to the boxed areas in G but in higher magnification; H′ and H″ correspond to the boxed areas in H. An upregulation of Fibronectin was detected in the dorsal and hindgut mesentery in *Msx1*$^{-/-}$;*Msx2*$^{-/-}$ mutants compared to their littermate controls. (I) RT-PCR analysis confirmed the above observations

by revealing a higher relative mRNA level of *Fn* in the mutants (asterisk, P<0.005). HG, hindgut; GR, genital ridge; DA, dorsal aorta; DM, dorsal mesentery.